Anal. Chem. **1998,** *70,* 4339−4343

An Oscillometric Detector for Capillary Electrophoresis

José A. Fracassi da Silva and Claudimir L. do Lago*

Departamento de Química Fundamental, Instituto de Química, Universidade de São Paulo, Av. Prof. Lineu Prestes 748, CEP 05508-900, São Paulo, Brazil

An oscillometric detector for capillary electrophoresis (CE) has been described. Two 2-mm silver rings separated by 1 mm were painted over the polyimide coating of a fused-silica capillary (75-μm i.d. and 360-μm o.d.) and used as electrodes for oscillometric measurements. A function generator was used to apply a sinusoidal signal over one of the electrodes; the other one was connected to a current-to-voltage converter. The rectified signal is proportional to the admittance of the cell, which is a function of the inner solution conductivity in the region of the electrodes. Electropherograms of alkaline and alkaline-earth cations showed good signal-to-noise ratio. For typical electrophoretic conditions, the limit of detection for lithium was 1.5 μM, and there was good linearity ($R = 0.998$ for eight data points) up to 2 mM. Indirect conductivity detection of quaternary ammonium salts was achieved by using potassium acetate running buffer, showing results similar to those from conventional conductometric detectors. Despite the cell length (5 mm), good resolution was obtained in the electropherograms. Equivalent electrical circuits were proposed for the cell. The most simplified model comprises a resistor−capacitor couple in parallel with another capacitor. The resistor stands for the inner solution resistivity, the series capacitor stands for the fused-silica wall dielectric properties in the region between the electrodes and the solution, and the parallel capacitor stands for the leakage through the wall and edge capacitance effects.

Since the introduction of capillary electrophoresis (CE),[1,2] a great variety of detection systems have been proposed. The choice of the detection scheme is made by taking into account several requirements, among them the selectivity. A more specific detector may be used to overcome unresolved peaks. On the other hand, a detector with low specificity may be the best choice when there are no problems with peak separations. This second case made the conductometric detector the most used one in ion chromatography. However, the high electric field inside the column and the difficulty in positioning electrodes are important drawbacks of this detection mode for CE.

The conductometric detectors for CE were inspired by the devices used in chromatography and isotachophoresis. Mikkers and co-workers used the fluctuations of the potential gradient inside the column, which is a mode of conductometric detection.[1]

In early works, PTFE capillaries with sizable inner diameter were employed, which allowed some ease in the construction and positioning of the electrodes. However, this is not an easy task for the current fused-silica capillaries. A CO_2 laser has been used by Zare and co-workers to drill fused-silica capillaries.[3,4] Although small and precise holes may be obtained by this procedure, the CO_2 laser is an expensive apparatus. An alternative is the end-column configuration, in which the electrodes are positioned near the end of the capillary.[5−9] Difficulties in the spatial positioning and dead volume are possible drawbacks of this approach.

To overcome the interference of the electric field involved in the CE, a suppressor column, similar to that of ion chromatography, may be used.[10−13] The ground electrode is placed in the regenerate electrolyte, which eliminates the strong electric field from that point to the end of the column, where the conductivity detector is positioned. Suppression of the background conductivity is an additional advantage of this approach which enhances the sensitivity. On the other hand, there is an additional broadening of the peaks.

In this work, an oscillometric detector is presented. It resembles old apparatuses for this kind of measurement,[14] but with dimensions to fit capillary electrophoresis and with new electronics. Basically, two ring electrodes are positioned outside the column over a 5-mm region near the grounded end of the

* To whom correspondence should be addressed. Fax: +55 11 818 3837. E-mail: claudemi@iq.usp.br.

(1) Mikkers, F. E. P.; Everaerts, F. M.; Verheggen, Th. P. E. M. *J. Chromatogr.* **1979**, *169*, 1−10.
(2) Jorgenson, J. W.; Lukacs, K. D. *Anal. Chem.* **1981**, *53*, 1298−1302.
(3) Huang, X.; Pang, T.-K. J.; Gordon, M. J.; Zare, R. N. *Anal. Chem.* **1987**, *59*, 2747−2749.
(4) Huang, X.; Luckey, J. A.; Gordon, M. J.; Zare, R. N. *Anal. Chem.* **1989**, *61*, 766−770.
(5) Huang, X.; Zare, R. N.; Sloss, S.; Ewing, A. G. *Anal. Chem.* **1991**, *63*, 189−192.
(6) Huang, X.; Zare, R. N. *Anal. Chem.* **1991**, *63*, 2193−2196.
(7) Kar, S.; Dasgupta, P. K.; Liu, H.; Hwang, H. *Anal. Chem.* **1994**, *66*, 2537−2543.
(8) Haber, C.; Jones, W. R.; Soglia, J.; Surve, M. A.; McGlynn, M.; Caplan, A.; Reineck, J. R.; Krstanovic, C. *J. Cap. Electrophor* **1996**, *3*, 1−11.
(9) Müller, D.; Jelínek, I.; Opekar, F.; Štulík, K. *Electroanalysis* **1996**, *8*, 722−725.
(10) Dasgupta, P. K.; Bao, L. *Anal. Chem.* **1993**, *65*, 1003−1011.
(11) Dasgupta, P. K.; Kar, S. *Anal. Chem.* **1995**, *67*, 3853−3860.
(12) Avdalovic, N.; Pohl, C. A.; Rocklin, R. D.; Stillian, J. R. *Anal. Chem.* **1993**, *65*, 1470−1475.
(13) Harrold, M.; Stillian, J.; Bao, L.; Rocklin, R.; Avdalovic, N. *J. Chromatogr. A* **1995**, *717*, 371−383.
(14) Burkhalter, T. S. High-Frequency Conductometric (Impedimetric) Titrations. In *Comprehensive Analytical Chemistry IIA—Electrical Methods*; Wilson, C. L., Wilson, D. W., Eds.; Elsevier: Amsterdam, 1964; Chapter V.

S0003-2700(98)00185-1 CCC: $15.00
Published on Web 09/10/1998

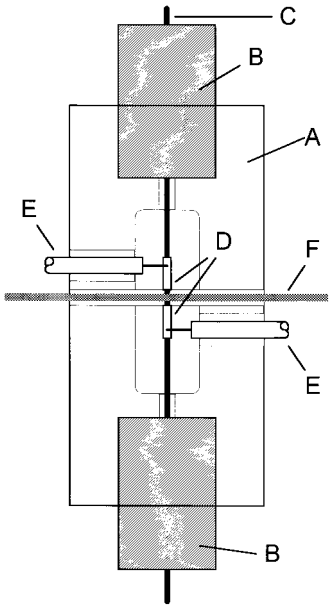

Figure 1. Oscillometric cell. (A) Plexiglas base, (B) silicone septa, (C) fused-silica capillary, (D) silver paint ring (electrode), (E) electrode terminal, (F) ground plane.

fused-silica capillary. A high-frequency signal is applied over the electrodes, and the resulting current that passes through the cell is amplified, rectified, and measured. This current is a function of the admittance. Since the column is filled with an aqueous solution of electrolyte, the measured admittance is a function of the conductance in the region between the electrodes. Thus, this detector may be intended as a contactless conductometric detector.

Chromatography and isotachophoresis have been contemplated with contactless detectors,[15−17] and recently Zemann and co-workers proposed a similar scheme of detection for CE.[18] The present work describes a detector for CE which has some advantages over this one, such as sensitivity and cell size.

EXPERIMENTAL SECTION

Cell Construction. The electrodes were made by painting two rings of silver paint (Cerdec, Americana, Brazil) over the polyimide coating at 2 cm from the end of a 54-cm fused-silica capillary (75-μm i.d. and 360-μm o.d.) (J & W Scientific, Folsom, CA). Silver paint was also used to attach the wires from the electronic circuit. A Plexiglas piece and two silicone septa hold this region of the capillary, as shown in Figure 1. A ground plane is inserted between the electrode to minimize capacitive leakage. This ground plane was made of a piece of Tetra Rex package (Tetra Pak, Monte Mor, Brazil), from a commercial package of fruit juice, with a 0.4-mm-diameter central hole to pass the capillary. This package material is comprised of paper, aluminum, and polyethylene sheets with thicknesses of 0.50, 0.01, and 0.04 mm, respectively. The edge of the aluminum sheet was exposed by heating the polyethylene film and then connected to ground of the circuit.

Electronic Circuit. Figure 2 shows the diagram of the electronic circuit. A function generator FG-2002C (Goldstar, Seoul, Korea) generates a 600-kHz 20-V_{pp} sinusoidal signal. This signal is applied to one of the electrodes. The other one is connected to the input of a current-to-voltage converter. The current-dependent voltage is rectified, and the last stage (A3) amplifies the signal and compensates the baseline.

The best frequency of operation may be optimized, depending on the actual dimensions of the capillary and electrodes, as well as the quality of the electronic parts used. In this last case, the critical component is the operational amplifier A1, which operates at a relatively high frequency and a low input current.

CE Apparatus. A homemade CE system was used. It consists basically of a thermostated Plexiglas case, a 0−30-kV power supply (Glassman, Whitehouse Station, NJ), and an interfaced 386 microcomputer. The PCL711B interface (Advantech, Taipei, Taiwan) allows the microcomputer to control the high-voltage power supply through a 12-bit digital-to-analog converter and to monitor the current, the case temperature, and the detector signal through a 12-bit analog-to-digital converter. For operator safety, the capillary, buffer reservoirs, electrodes, and detection cell were all enclosed in the Plexiglas case, which was equipped with an interlock switch on the access door.

Solutions and Reagents. All solutions were prepared with Nanopure deionized water, and all the chemicals were of reagent grade and used as received. Solutions with alkaline and alkaline-earth cations were prepared by dilution of 100 mM stock solutions of KCl, NaCl, $BaCl_2$, $CaCl_2$, $MgCl_2$, and LiCl. Tetramethylammonium (TMA^+), tetrabutylammonium (TBA^+), and tetraethylammonium (TEA^+) 50 mM stock solutions were prepared from their bromide salts. Benzyltriethylammonium ($TEBA^+$) 50 mM stock solution was prepared from its chloride salt. For direct conductivity detection, running buffers were prepared by dilution of a 100 mM stock solution of 2-[*N*-morpholino]ethanesulfonic acid (MES) and histidine (His) without pH adjustment. Indirect conductivity detection was carried out in potassium acetate running buffer prepared by dilution of a 100 mM stock solution and adjustment with acetic acid to pH 5.2.

RESULTS AND DISCUSSION

Figure 3 shows an electropherogram of a 10 μM solution of potassium, barium, calcium, sodium, magnesium, and lithium, which migrated in this sequence, in a 10 mM MES/His running buffer (pH 6.0). Gravity injection from 100 mm for 30 s was performed and the detector operated at nonoptimized frequency of 600 kHz. Due to its low mobility, lithium has the lowest response factor among the above-cited cations. For the same electrophoretic conditions, the estimated limit of detection for lithium was 1.5 μM, and good linearity ($R = 0.998$ for eight data points) was obtained up to 2 mM. Since the concentration of the running buffer is 20 mM, analyte concentrations above 2 mM were not evaluated. The limits of detection for the other cations are 1.1, 1.2, 1.4, 1.6, and 1.2 μM for K^+, Ba^{2+}, Ca^{2+}, Na^+, and Mg^{2+}, respectively.

Indirect conductivity detection may also be performed, as shown in Figure 4. As expected, due to the low mobility of the TMA^+, TEA^+, $TEBA^+$, and TBA^+ when compared to the potassium from the running buffer (5 mM potassium acetate, pH 5.2),

(15) Pál, F.; Pungor, E.; Kováts, E. *Anal. Chem.* **1988**, *60*, 2254−2258.
(16) Gaš, B.; Demjanìnko, M.; Vacík, J. *J. Chromatogr.* **1980**, *192*, 253−257.
(17) Vacík, J.; Zuska, J.; Muselasová, I. *J. Chromatogr.* **1985**, *320*, 233−240.
(18) Zemann, A. J.; Schnell, E.; Volgger, D.; Bonn, G. K. *Anal. Chem.* **1998**, *70*, 563−567.

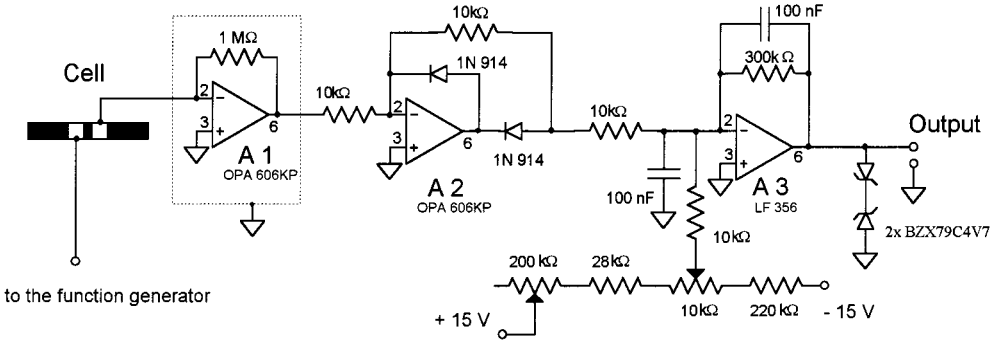

Figure 2. Electronic circuit. The current-to-voltage converter A1 is kept in a grounded metallic case placed as near as possible to the cell. A2 and related components compose a precision rectifier. The adjustable resistors compensate the baseline before a 30× gain is applied by A3 to the dc signal. The back-to-back zener diodes protect the A/D converter against overvoltage.

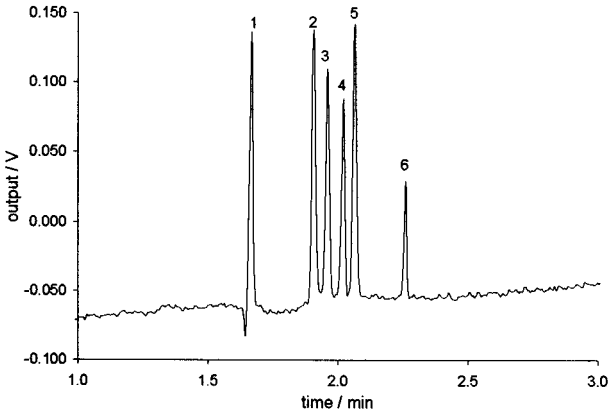

Figure 3. Electropherogram of a 10 μM solution of potassium (1), barium (2), calcium (3), sodium (4), magnesium (5), and lithium (6) in a 10 mM MES/His running buffer (pH 6.0). Gravity injection from 100 mm for 30 s was performed, and the detector was operated at 600 kHz.

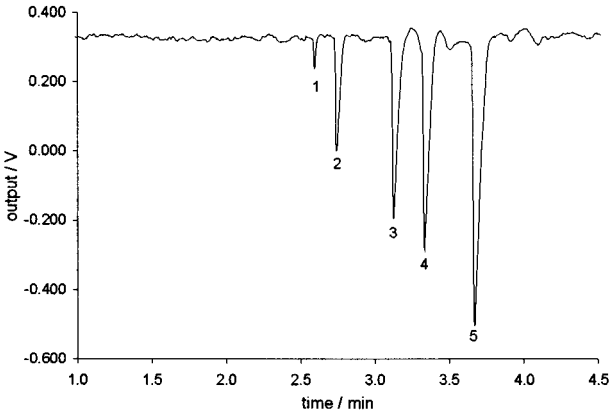

Figure 4. Electropherogram of a 50 μM solution of TMA^+ (2), TEA^+ (3), $TEBA^+$ (4), and TBA^+ (5) in a 5 mM potassium acetate running buffer (pH 5.2). Peak 1 is a system peak. Hydrodynamic injection from 100 mm for 30 s was performed, and the detector was operated at 600 kHz.

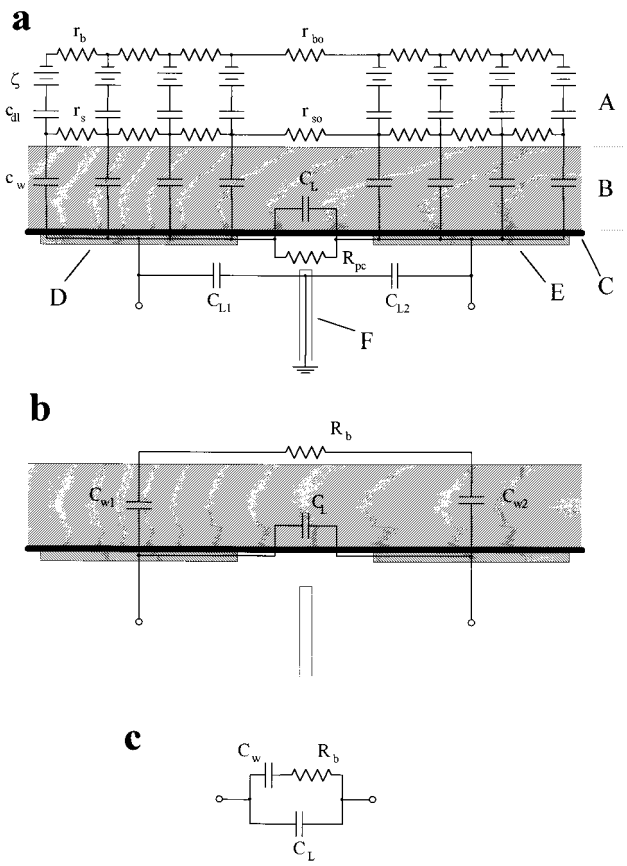

Figure 5. Equivalent circuits for the cell. The interior of the capillary (A), fused-silica wall (B), polyimide coating (C), electrodes (D and E), and ground plane (F) are considered in the models. A first model is proposed in panel a, where c_w, c_{dl}, ζ, r_s, and r_b are infinitesimal components standing for the wall capacitance, double-layer capacitance, ζ potential, resistance of the inner surface of the capillary, and bulk solution resistance, respectively; r_{bo}, r_{so}, and R_{pc} are the resistances of the bulk of the solution, inner surface of the capillary, and polyimide coating between the electrodes, respectively; C_{L1} and C_{L2} are the capacitances between each electrode and the ground plane; and C_L stands for generic leakages between the electrodes (edge effect, for example). A simple model is proposed in panel b, where R_b stands for the solution resistance in the region of the electrodes and C_{w1} and C_{w2} are the capacitances due to the capillary wall. These capacitances may be combined, resulting in the simplest model, proposed in panel c.

negative peaks were obtained, and their magnitudes were proportional to their migration times. Due to the high conductivity of the potassium acetate running buffer, the baseline is not as stable as that obtained for MES/His. The limits of detection for TMA^+, TEA^+, $TEBA^+$, and TBA^+ were 10.4, 6.6, 5.5, and 4.2 μM, respectively.

To explain the operation of the detector, equivalent electrical circuits were proposed. Taking into account the components proposed by Ewing and co-workers,[19] it is possible to suggest the model shown in Figure 5a. In this case, a network composed of infinitesimal-length resistors, capacitors, and batteries was used

to represent the region enclosed by each electrode. A simplified model may be proposed which allows one to get some insight about the global behavior of the detector. Since there is a capacitive barrier (fused silica) in series with the battery (the ζ potential) and an alternate signal is used, the dc contribution of this battery may be disregarded. The high-frequency signal needed to reduce the impedance of the silica wall to the order of magnitude of the bulk solution resistance certainly makes the impedance of the double layer small when compared with the bulk solution resistance. Thus, this component is disregarded, and the bulk solution and superficial resistors are in parallel. The polyimide resistance is large enough and may be ignored. Considering that the oscillator has a low output impedance and is connected to the electrode D, the capacitor C_{L1} is not important. The last approximation is to consider that the RC network may be represented by only one resistor and one capacitor. The capacitor C_{L2} is in parallel with the input capacitance of the current-to-voltage converter (~3 pF for the OPA606KP operational amplifier). Thus, it causes an extra, but small, reduction of the frequency bandwidth and may be included in the whole performance of the circuit. The resulting circuit is shown in Figure 5b. Figure 5c shows the final equivalent circuit, which is used in further discussions.

Further important information to understand the detector is the frequency response of the current-to-voltage converter, which is the critical part of the electronic circuit. Figure 6a shows the response of this converter in the range between 10 and 1000 kHz. The transition frequency is determined by the operational amplifier as well as by the other components and the layout of the printed circuit board.

The equivalent circuit from Figure 5c allows us to conclude that, due to the capacitor C_L, the baseline would be increased with the frequency. However, due to the limited frequency bandwidth of the current-to-voltage converter, the baseline would be decreased after the frequency transition. This was experimentally observed (Figure 6b).

The equivalent circuit also shows that the impedance of the couple R_bC_w would tend to the solution resistance with increasing frequency, which is highly beneficial because the impedance of the cell would be mainly dependent on the conductivity of the inner solution in the region of the cell. However, again due to the limited performance of the current-to-voltage converter, a maximum value is obtained (Figure 6c).

Although the aspects described above can be easily understood through the proposed model, the signal-to-noise ratio (SNR) as a function of the frequency cannot be straightforwardly obtained from the simplified model. Figure 6d shows that the SNR is not a well-behaved function of the frequency. Of course, this profile is not only due to the conductivity of the solution but also results from the combination with the noises due to the dielectric properties of the fused silica wall as well as the other components of the electronic circuit. It is important to note that the frequency for the maximum peak area does not correspond to the maximum SNR. At the best frequency of operation dictated by the SNR (800 kHz), the peaks have area ~26% of those at the maximum peak area frequency. On the other hand, the SNR is ~2 times greater.

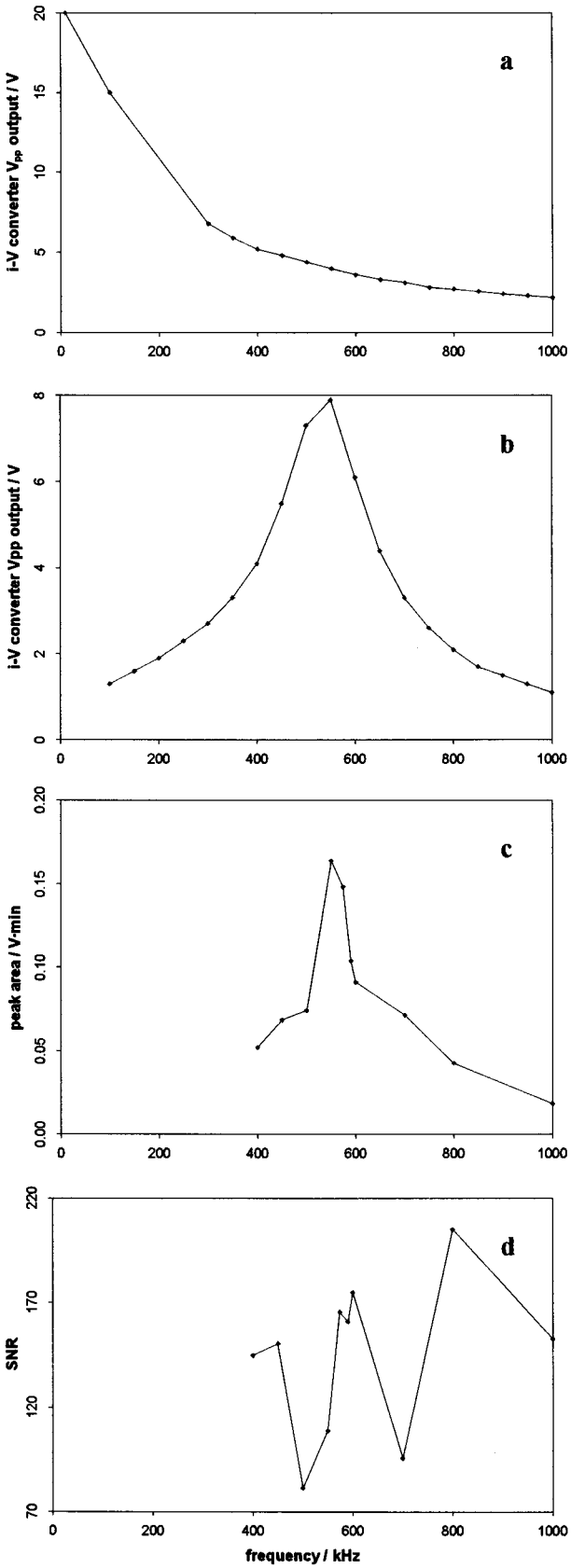

Figure 6. Response of the detector as a function of the operating frequency: (a) peak-to-peak voltage at the output of the current-to-voltage converter with a resistive dummy cell (10 kΩ); (b) the same as in (a), but with the cell and the capillary filled with 10 mM MES/His buffer; (c) peak area of 80 μM K^+ in 10 mM MES/His running buffer; (d) SNR for the peaks of (c).

(19) Hayes, M. A.; Kheterpal, I.; Ewing, A. G. *Anal. Chem.* **1993**, *65*, 2010−2013.

Thus, the operation frequency is an important parameter, but unfortunately the best value is not easily determined.

For the included examples, the estimated length of the sample plug was about 10 mm, which is double the cell length (5 mm). Despite this large cell length, when compared with other conductometric detectors,[3] the detector has advantages such as the electrical isolation between inner solution and detector provided by the fused-silica wall, simplicity of construction, and robustness. Moreover, even when working at a frequency, much higher than those of conventional conductivity detectors, the electronic circuit is simple and inexpensive. Although electrophoretic conditions were not optimized, as well as the operating frequency of the detector, good resolution and SNR were achieved, which suggests that this detector may be useful in many applications.

ACKNOWLEDGMENT

This work was supported by the Conselho Nacional de Desenvolvimento Científico e Tecnológico (PADCT/CNPq) and Fundação de Amparo à Pesquisa do Estado de São Paulo (FAPESP). The authors thank CNPq for the research fellowships and Dr. Marina F. M. Tavares from Instituto de Química—USP. This work was presented at The Third Latin-American Symposium on Biomedical, Biopharmaceutical, and Industrial Applications of Capillary Electrophoresis, Buenos Aires, Argentina, 1997.

Received for review February 17, 1998. Accepted July 28, 1998.

AC980185G